Otology & Neurotology
29:513–517 © 2008, Otology & Neurotology, Inc.

Detection of Postoperative Residual Cholesteatoma With Non-Echo–Planar Diffusion-Weighted Magnetic Resonance Imaging

*Bert De Foer, †Jean-Philippe Vercruysse, *Anja Bernaerts, *Filip Deckers, *Marc Pouillon, †Thomas Somers, *‡Jan Casselman, and †Erwin Offeciers

*Departments of *Radiology and †ENT, Augustinus Hospital, Wilrijk (Antwerp); and ‡Department of Radiology, AZ Sint-Jan AV Hospital, Bruges, Belgium*

Objective: The aim of this study was to analyze the role of non–echo-planar imaging (non-EPI)–based diffusion-weighted (DW) magnetic resonance imaging (MRI) for the detection of residual cholesteatoma after canal wall-up mastoidectomy before eventual second-look surgery.
Study Design: Prospective and blinded study.
Setting: Tertiary referral center.
Patients: The study group included the surgical, clinical, and imaging follow-up of 32 consecutive patients after primary cholesteatoma surgery.
Interventions: All patients were investigated with MRI, including late postgadolinium T1-weighted sequence and non-EPI-DW sequence, 10 to 18 months after first-stage cholesteatoma surgery by experienced surgeons using a canal wall-up mastoidectomy. The non–EPI-DW images were evaluated for the presence of a high–signal intensity lesion consistent with residual cholesteatoma. Imaging findings were correlated with findings from second-stage surgery in 19 patients, clinical follow-up examination in 11 patients, and, in 2 patients, clinical and MRI follow-up examination.
Results: Non–EPI-DW sequences depicted 9 of 10 residual cholesteatomas. The only lesion missed was a 2-mm cholesteatoma in an examination degraded by motion artifacts in a child. All other diagnosed cholesteatomas measured between 2 and 6 mm. Sensitivity, specificity, positive predictive value, and negative predictive value were 90, 100, 100, and 96%, respectively.
Conclusion: Except for motion artifact–degraded examinations, non–EPI-DW MRI is able to detect even very small residual cholesteatoma after first-stage surgery by showing a high–signal intensity lesion. It has the capability of selecting patients for second-look surgery, avoiding unnecessary second-look surgery. **Key Words:** Cholesteatoma—Diffusion weighted—Middle ear—MRI.
Otol Neurotol **29:**513–517, 2008.

Surgical treatment of an acquired middle ear cholesteatoma can be performed by a canal wall-up (CWU) procedure, but this carries the risk of leaving residual cholesteatoma behind (1–4).

The detection of residual cholesteatoma after CWU techniques with the use of computed tomography has been shown to be inaccurate (5–7). Recent reports, however, suggested an improvement in magnetic resonance imaging (MRI) technique in diagnosing cholesteatoma using delayed contrast-enhanced T1-weighted imaging (8–9) and echo-planar diffusion-weighted (EPI-DW) sequences (10–13). However, EPI-DW imaging still has a size limit of 5 mm in visualizing postoperative middle ear cholesteatoma due to its low resolution, thicker slices, and susceptibility artifacts (10,12,13). Therefore, EPI-DW sequences seem to be useless for the detection of the usually quite small residual cholesteatoma (13). Very recently, the use of non–EPI-based DW sequences has been described for the detection of middle ear cholesteatoma (14) and postoperative recurrent cholesteatoma (15). These turbo spin-echo (TSE) DW sequences have a higher imaging matrix, thinner slice thickness, and—more importantly—a complete lack of susceptibility artifacts. The purpose of this study was to evaluate the sensitivity and specificity of a single-shot (SS) TSE DW sequence in detecting residual cholesteatoma after first-stage cholesteatoma surgery.

Address correspondence and reprint requests to Bert De Foer, M.D., Department of Radiology, St.-Augustine Hospital, Oosterveldlaan 24, 2610 Wilrijk (Antwerp), Belgium; E-mail: bert.defoer@GZA.be

PATIENTS AND METHODS

Patients

Between July 2005 and April 2007, we investigated 32 consecutive patients (22 men and 10 women; age range, 7–71 yr; mean age, 39.4 yr) in a blinded and prospective study. Institutional

review board approval and informed consent were not required. All patients had undergone first-stage cholesteatoma surgery between 10 and 18 months earlier and were clinically followed by micro-otoscopy and audiometry. All patients had computed tomographic (CT) and MRI evaluation regardless of their previous first-stage surgical findings. Both readers were blinded to the clinical information of the patient, first-stage surgical findings, and CT findings. The decision to perform second-look surgery was made by the ear, nose, and throat surgeon and was based upon the findings during first-stage surgery. The decision not to stage reflected the surgeon's evaluation of having completely removed cholesteatoma at the first stage in patients with easily dissected less extensive disease. In 19 patients, a second stage was performed either as a planned stage to check for residual disease in the patients with more extensive cholesteatoma or as a functional second stage in patients with remaining conductive hearing loss. All patients were regularly observed for a clinical follow-up, including micro-otoscopy and audiometry. The remaining 13 patients, with limited cholesteatoma extension during first-stage surgery and reassuring clinical and otoscopic findings, were observed for clinical follow-up examination, including micro-otoscopy and audiometry. Two of these clinically negative patients received further MRI follow-up examinations, including late postgadolinium T1-weighted and SS TSE DW imaging. Surgical findings, including exact location of the residual cholesteatoma, were obtained from surgical reports.

Imaging Technique

Computed tomographic scanning was performed on a 16-row multislice CT scan (Lightspeed, GE, Milwaukee, WI, USA) using an axial volume scan (140 kV, 250 mA, 1-s rotation, 5.62 pitch, high-resolution bone algorithm) with coronal reconstruction. Axial slices were acquired with a thickness of 0.625 mm, centered in a 9.6-cm field of view on the right and left ear, with a reconstruction interval of 0.2 mm.

Magnetic resonance imaging was performed on a 1.5-T superconductive unit (Magnetom Avanto; Siemens Medical Solutions, Erlangen, Germany) using the standard Head Matrix coil. Axial 2-mm-thick spin-echo T1-weighted images (repetition time [TR], 400 ms; time to echo [TE], 17 ms; matrix, 192 × 256; field of view, 150 × 200 mm), and coronal 2-mm-thick spin-echo T1-weighted images were acquired with the same parameters except for the matrix, which was set at 144 × 256 for the coronal images. Coronal 2-mm-thick TSE T2-weighted images (TR, 3,500 ms; TE, 92 ms; matrix, 192 × 256; field of view, 150 × 200 mm) and axial 0.4-mm-thick 3-dimensional TSE T2-weighted images (TR, 1,500 ms; TE, 303 ms; matrix, 228 × 448; field of view, 107 × 210 mm) were also performed. In all patients, a 2-mm-thick SS TSE DW sequence was acquired in the coronal plane (TR, 2,000 ms; TE, 115 ms; matrix, 134 × 192; field of view, 220 × 220 mm; b factors, 0 and 1,000 mm^2/s). The coronal plane was preferred more than the axial plane because in the past, using EPI-DWI, the coronal plane showed less artifacts.

TABLE 1. *Summarized findings of the 19 patients who underwent second-look surgery*

No.	Side	Age, yr	Aeration ME	Aeration POC	Surgical findings	SS TSE DWI	Size, mm
1	L	37.5	+	−	Positive	Positive	2
2	R	48.2	+	+/−	Negative	Negative	—
3	L	37.2	+	+/−	Negative	Negative	—
4	R	34.5	+	−	Negative	Negative	—
5	R	6.7	+	−	Negative	Negative	—
6	L	23.8	−	−	Negative	Negative	—
7	L	55.2	−	−	Negative	Negative	—
8	R	43.1	−	−	Negative	Negative	—
9	R	41.9	+/−	−	Positive	Positive	4
10	L	5.7	−	−	Positive	Negative	2
11	L	39.2	+	+	Positive	Positive	2.5
12	L	69.9	+	−	Negative	Negative	—
13	R	47.2	+	+/−	Negative	Negative	—
14	L	23.2	+	+	Positive	Positive	4
15	R	50.9	+	+	Positive	Positive	3
16	R	43.5	+	+	Positive	Positive	4
17	L	17.5	+	+	Positive	Positive	6
18	R	35.0	+	+	Positive	Positive	3
19	R	45.7	+	−	Positive	Positive	4

Thirteen patients followed by otoscopy and imaging are not outlined in this table (see text for further details).

— indicates no data available; aeration ME (+), aerated middle ear cavity; aeration ME (−), opacified/nonaerated middle ear cavity; aeration ME (+/−), partial aeration of the middle ear cavity; aeration POC (+), aerated postoperative cavity; aeration POC (−), opacified/nonaerated postoperative cavity; aeration POC (+/−), partial aeration of the postoperative cavity; L, left; R, right; SS TSE DWI, single-shot turbo spin-echo diffusion-weighted magnetic resonance imaging; SS TSE DWI (+), presence of a clear hyperintensity; SS TSE DWI (−), absence of a clear hyperintensity.

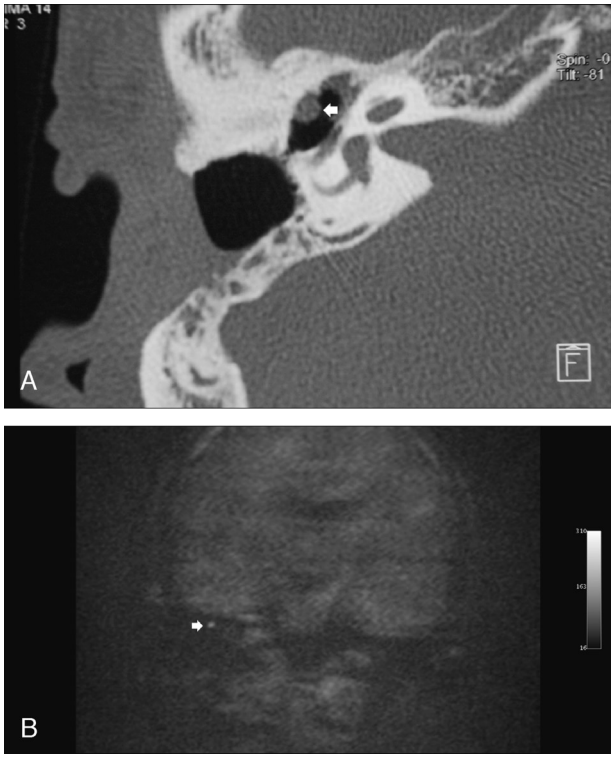

FIG. 1. A 35-year-old man evaluated 13 months after cholesteatoma surgery before second-look surgery. Second-look surgery demonstrated a 3-mm small residual cholesteatoma (Case 18). *A*, Axial CT scan demonstrates the small soft tissue nodule at the anterior epitympanic space consistent with the small residual cholesteatoma (*arrow*). *B*, Coronal SS TSE DW sequence showing the cholesteatoma as a very small nodular hyperintense lesion (*arrow*) in the signal void of the right temporal bone under the right temporal lobe. The diagnosis of the cholesteatoma in an aerated middle ear and cavity can be equally performed by the SS TSE DW sequence as by the CT scan.

All sequences were acquired 45 minutes after intravenous contrast injection of 0.1 mmol/kg of body weight of gadoterate meglumine (Dotarem; Guerbet, Roissy, France) or gadopentetate dimeglumine (Magnevist; Schering, Berlin, Germany).

Image Interpretation

Images were evaluated prospectively in consensus by 2 experienced head and neck radiologists blinded to the results of first-stage surgery and clinical and CT data of the patient.

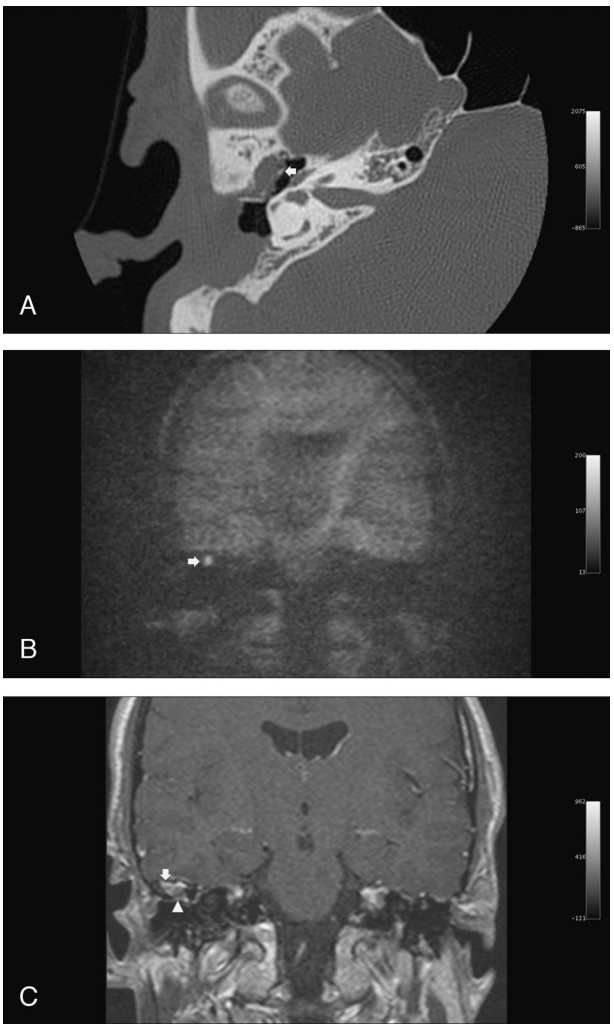

FIG. 2. A 42-year-old man evaluated 17 months after first-stage cholesteatoma surgery before second-look surgery. Second-look surgery demonstrated a 4-mm small anterior epitympanic residual cholesteatoma in a postoperative cavity filled with scar tissue (Case 9). *A*, Axial CT scan. A status after CWU mastoidectomy is found with a partial opacification of the middle ear and postoperative cavity. It is impossible to locate the cholesteatoma on these images. When correlated with MRI, a nodular soft tissue lesion in the anterior epitympanic space can be suspected (*arrow*). *B*, Coronal SS TSE DW sequence showing a small nodular hyperintense lesion (*arrow*) under the tegmen in the signal void of the right temporal bone, consistent with the small residual cholesteatoma. *C*, Coronal late postgadolinium SE T1-weighted image (same slice position as *B*). The cholesteatoma is observed as a small nodular nonenhancing lesion (*arrowhead*) surrounded by enhancing postoperative and inflammatory tissue (*arrow*).

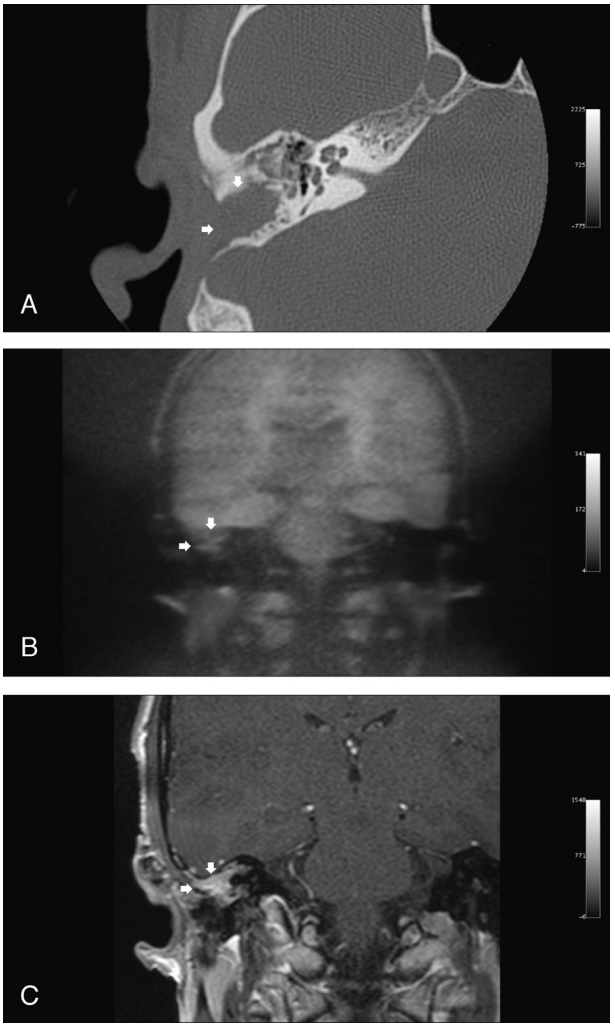

FIG. 3. A 35-year-old man evaluated 12 months after first-stage cholesteatoma surgery before second-look surgery. Second-look surgery demonstrated postoperative and inflammatory changes without any evidence of residual cholesteatoma (Case 4). *A*, Axial CT scan. A status after CWU mastoidectomy is noted. Complete opacification of the postoperative cavity can be found (*arrows*). No differentiation of these soft tissues can be made. *B*, Coronal SS TSE DW sequence. No clear nodular hyperintense lesions can be observed excluding residual cholesteatoma (compared with the signal intensity of the residual cholesteatoma in Figs. 1B and 2B). Note the moderately intense signal of the inflammatory and postoperative changes in the cavity (*arrows*).*C*, Coronal late postgadolinium T1-weighted image. Enhancement of the inflammatory and postoperative changes in the cavity can be noted (*arrows*).

The SS TSE DW sequences were evaluated first. Turbo spin-echo T2 and late postgadolinium T1-weighted sequences were evaluated afterward for correlation with the SS TSE DW sequences. Single-shot TSE DW images were considered positive for cholesteatoma if a nodular hyperintense lesion was observed. On the TSE T2 images, a cholesteatoma was diagnosed in case of a nodular moderately intense lesion, with a corresponding nonenhancing or rim-enhancing lesion on the late postgadolinium T1-weighted images.

TABLE 2. *Sypnosis of the major published references on magnetic resonance imaging of cholesteatoma*

Authors	Cholesteatoma type	MR technique	n	Size limit, mm	Sensitivity, %	Specificity, %	PPV, %	NPV, %
Fitzek et al. (11)	Primary acquired	EPI-DWI	15	—	—	—	—	—
Aikele et al. (10)	Recurrent	EPI-DWI	22	5	77	100	100	75
Ayache et al. (9)	Residual	Late post-Gd T1-WI	41	3	90	100	100	92
Stasolla et al. (12)	Residual/recurrent	EPI-DWI	18	5	86	100	100	92
Vercruysse et al. (13)	Primary acquired	EPI-DWI	55	5	81	100	100	40
Vercruysse et al. (13)	Residual	EPI-DWI	45	5	12.5	100	100	72
Dubrulle et al. (15)	Recurrent	Non–EPI-DWI	24	5	100	91	93	100
De Foer et al. (19)	Primary acquired	Non–EPI-DWI	21	2	—	—	—	—

— indicates no data available; EPI-DWI, echo-planar diffusion-weighted imaging; late post-Gd T1-WI, late postgadolinium enhanced T1-weighted imaging; non–EPI-DWI, non–echo-planar diffusion-weighted imaging; NPV, negative predictive value; PPV, positive predictive value.

An aerated middle ear and postoperative cavity were diagnosed if the homogeneous signal loss of the temporal bone—caused by air and bone—can be observed on late postgadolinium T1-weighted and on T2-weighted MR images. In case of postoperative and/or inflammatory changes, a lack of hyperintensity on SS TSE DW images, a complete enhancement on late postgadolinium T1-weighted sequences, and a clear hyperintense signal on T2-weighted images were observed. All examinations were classified as either positive or negative for cholesteatoma. The greatest diameter of the cholesteatoma was measured.

Statistical Evaluation

The sensitivity, specificity, and negative and positive predictive values were calculated.

RESULTS

Of the 19 patients who underwent surgery, 18 were proven to have the correct diagnosis on the basis of the SS TSE DW sequence alone. There were true-positive findings for cholesteatoma in 9 patients. The cholesteatoma size varied between 2 and 6 mm (Table 1). Of these 9 true-positive patients, 6 showed a surrounding signal void on standard MRI sequences corresponding to a well-aerated postoperative cavity (Fig. 1B). In the remaining 3 true-positive patients, the cholesteatoma was embedded in postoperative and/or inflammatory changes (Fig. 2, B and C). On computed tomography, only the residual cholesteatoma in an aerated middle ear and postoperative cavity can be visualized (Fig. 1A), whereas the residual cholesteatoma embedded in an opacified middle ear and postoperative cavity could not be discerned (Fig. 2A).

True-negative findings were recorded in 9 patients. In all these patients, the mastoidectomy cavity was completely or partially filled with postoperative and/or inflammatory changes. On computed tomography, it was impossible to exclude any residual cholesteatoma (Fig. 3A).

In 1 motion-artifact–degraded examination, a 2-mm small cholesteatoma pearl was missed on all sequences, resulting in 1 false-negative case (Case 10). There were no false-positive cases.

Thirteen patients had limited cholesteatoma extension during first-stage surgery, allowing for easy, total eradication of the disease. In these patients, no second-stage surgery was performed, and the clinical follow-up and audiometry were reassuring. Micro-otoscopy showed an intact postoperative tympanic membrane or graft without a retraction pocket. In this subgroup, no nodular hyperintensities were found on SS TSE DW images. In 4 of these patients, extensive postoperative scarring was observed on computed tomography with complete or partial opacification of the middle ear and postoperative cavity. In 9 patients, a signal void was noted on T1- and T2-weighted images corresponding with an aerated and disease-free middle ear and postoperative cavity.

All of these patients were interpreted as showing negative findings for cholesteatoma. The period of clinical follow-up ranged from 11.2 to 40.3 months, with a mean of 25.2 months.

Two patients received further MRI follow-up, including SS TSE DW, and late postgadolinium T1-weighted and T2-weighted sequences showing no hyperintensity on SS TSE DW. Sensitivity and specificity of SS TSE DWI were 90 and 100%, respectively. Positive and negative predictive values were 100 and 96%, respectively.

DISCUSSION

In our hospital, we perform the CWU technique for the treatment of middle ear cholesteatoma. This technique carries the risk of residual cholesteatoma behind, thus often requiring second-look surgery. Distinction should be made between residual and recurrent cholesteatoma. Residual cholesteatoma is defined as keratinizing epithelium left behind at the first stage that has regrown into a cholesteatoma pearl. Recurrent cholesteatoma is defined as newly developed cholesteatoma arising from a retraction pocket in the tympanic graft (16). The decision to perform second-stage surgery was based upon the surgical findings during first stage. The percentage of residual cholesteatoma in this current study is slightly higher than the number in the previously reported data from our ear, nose, and throat department (17–18) but substantially lower than the number of residual or recurrent cholesteatoma in literature, almost invariably reaching 50% (9,10,15). Computed tomographic scanning has been reported to be insufficient in detecting the presence of residual cholesteatoma after first-stage surgery (5–7). Several recent reports have highlighted mainly 2 MRI techniques in detecting primary, recurrent, and residual cholesteatoma (Table 2).

The technique of late postgadolinium T1-weighted sequences is able to detect residual cholesteatomas as small as 3 mm (8,9).

Other articles have highlighted the use and limitations of EPI-DW sequences for the demonstration of acquired middle ear cholesteatoma (11,13), residual (13), and recurrent (10,12) cholesteatoma.

Very recently, 2 articles have described non–EPI-DW sequences for imaging cholesteatoma (14,15). Dubrulle et al. (15) used a multishot TSE DW sequence in the detection of postoperative recurrent cholesteatoma. Despite the fact that this sequence has a lack of artifacts, a higher resolution, and a thinner slice thickness, the size limit for the detection of recurrent cholesteatoma in this study was analyzed at 5 mm, equaling the size limit for EPI-DW (10,12). In a technical report, we demonstrated the advantages of a SS TSE DW sequence over EPI DW: complete lack of susceptibility artifacts, thinner slices, and a higher imaging matrix (14).

In a recent study, we succeeded in demonstrating middle ear cholesteatoma as small as 2 mm in nonoperated ears using this SS TSE DW sequence (19).

In the 9 true-positive cases of the operated subgroup, SS TSE DW images correctly depicted residual cholesteatoma as a nodular hyperintense dot, with a size varying between 2 and 6 mm (Table 1). Correlation of these images to standard sequences made it possible to make the differentiation between a completely aerated middle ear/postoperative cavity and an opacified middle ear/postoperative cavity (Fig. 2). In aerated middle ears and postoperative cavities, SS TSE DW imaging equals computed tomography in detecting small residual cholesteatomas (Fig. 1). We conclude that the SS TSE DW sequence is far superior to EPI-DW sequences in detecting small residual postoperative cholesteatoma (Table 1).

In 9 cases, SS TSE DW images showed no hyperintensity leading to a true negative diagnosis, confirmed by second-stage surgery. It is clear that SS TSE DW allowed us to exclude cholesteatoma in these cases.

In 1 case, motion artifacts caused false-negative findings. In our previous study on SS TSE DW, we already mentioned motion artifacts as a possible cause of false-negative findings because in these cases, the hyperintensity of the small cholesteatoma is smeared out over multiple pixels, causing a lack of intensity (19). This is the reason why the small residual cholesteatoma was missed on the motion artifact–degraded examination in 1 child.

Our findings resulted in a sensitivity of 90% and a specificity of 100%. The positive predictive value was 100%, with a negative predictive value of 96%. If we do not take into account the examinations degraded by motion artifacts, the sensitivity even reaches 100%. This opens the possibility of screening for residual cholesteatoma by using the SS TSE DW sequence alone. We conclude that the SS TSE DW sequence is far superior to EPI-DW for the detection of residual middle ear cholesteatoma. Its high sensitivity, specificity, and positive and negative predictive value makes it possible to replace routine second-stage surgery for detection of residual cholesteatoma, thus avoiding unnecessary interventions.

Acknowledgments: The authors thank Johan Michiels, Siemens Medical Solutions Belgium, and Bernard Pilet for their help in the preparation of this article.

REFERENCES

1. Shelton C, Sheehy JL. Tympanoplasty: review of 400 staged cases. *Laryngoscope* 1990;100:679–81.
2. Stangerup SE, Drozdsiewicz D, Tos M, et al. Recurrence of attic cholesteatoma: different methods of estimating recurrence rates. *Otolaryngol Head Neck Surg* 2000;123:283–7.
3. Darrouzet V, Duclos JY, Portmann D, et al. Preference for the closed technique in the management of cholesteatoma of the middle ear in children: a retrospective study of 215 consecutive patients treated over 10 year. *Am J Otol* 2000;21:474–81.
4. Vartiainen E. Ten-year results of canal wall down mastoidectomy for acquired cholesteatoma. *Auris Nasus Larynx* 2000;21:227–9.
5. Tierney PA, Pracy P, Blaney SP, et al. An assessment of the value of the preoperative computed tomography scans prior to otoendoscopic "second look" in intact canal wall mastoid surgery. *Clin Otolaryngol Allied Sci* 1999;24:274–6.
6. Blaney SP, Tierney P, Oyarazabal M, et al. CT scanning in "second look" combined approach tympanoplasty. *Rev Laryngol Otol Rhinol (Bord)* 2000;121:79–81.
7. Wake M, Robinson JM, Witcombe JP, et al. Detection of recurrent cholesteatoma by computerized tomography after "closed cavity" mastoid surgery. *J Laryngol Otol* 1992;106:393–5.
8. Williams MT, Ayache D, Alberti C, et al. Detection of post-operative residual cholesteatoma with delayed contrast-enhanced MR imaging: initial findings. *Eur Radiol* 2003;13:169–74.
9. Ayache D, Williams MT, Lejeune D, et al. Usefulness of delayed postcontrast magnetic resonance imaging in the detection of residual cholesteatoma in the detection of residual cholesteatoma after canal wall-up tympanoplasty. *Laryngoscope* 2005;115:607–10.
10. Aikele P, Kittner T, Offergeld C, et al. Diffusion-weighted MR imaging of cholesteatoma in pediatric and adult patients who have undergone middle ear surgery. *AJR Am J Roentgenol* 2003;181:261–5.
11. Fitzek C, Mewes T, Fitzek S, et al. Diffusion-weighted MRI of cholesteatomas in petrous bone. *J Magn Reson Imaging* 2002;15:636–41.
12. Stasolla A, Magluilo G, Parrotto D, et al. Detection of postoperative relapsing/residual cholesteatoma with diffusion-weighted echo-planar magnetic resonance imaging. *Otol Neurotol* 2004;25:879–84.
13. Vercruysse JP, De Foer B, Pouillon M, et al. The value of diffusion-weighted MR imaging in the diagnosis of primary acquired and residual cholesteatoma: a surgical verified study of 100 patients. *Eur Radiol* 2006;16:1461–7.
14. De Foer B, Vercruysse JP, Pilet B, et al. Single-shot, turbo spin-echo, diffusion-weighted imaging versus spin-echo-planar, diffusion-weighted imaging in the detection of acquired middle ear cholesteatoma. *AJNR Am J Neuroradiol* 2006;27:1480–2.
15. Dubrulle F, Souillard R, Chechin D, et al. Diffusion-weighted MR imaging sequence in the detection of postoperative recurrent cholesteatoma. *Radiology* 2006;238:604–10.
16. Brackmann DE. Tympanoplasty with mastoidectomy: canal wall up procedures. *Am J Otol* 1993;14:380–2.
17. Schatteman I, Somers Th, Govaerts PJ, et al. Long term results of allograft tympanoplasty in adult cholesteatoma. Presented at the 6th International Conference on Cholesteatoma and Ear Surgery, Cannes, France, June 29–July 2, 2000.
18. Schilder AG, Govaerts PJ, Somers T, et al. Tympano-ossicular allografts for cholesteatoma in children. *Int J Pediatr Otolaryngol* 1997;18:31–40.
19. De Foer B, Vercruysse JP, Bernaerts A, et al. The value of single-shot turbo spin-echo diffusion-weighted MR imaging in the detection of middle ear cholesteatoma. *Neuroradiology* 2007;49:841–8.